3-2016

Harmonic analysis in integrated energy system based on compressed sensing

Ting YANG

Haibo PEN

Dan WANG

Zhaoxia WANG
Singapore Management University, zxwang@smu.edu.sg

Citation

1

Harmonic analysis in integrated energy system based on compressed sensing

Ting Yang[a], Haibo Pen[a], Dan Wang[a], Zhaoxia Wang[b]

[a] Key Laboratory of Smart Grid of Ministry of Education (Tianjin University), Tianjin 300072, China

[b] Institute of High Performance Computing, Agency for Science, Technology and Research, 138632, Singapore

Abstract

The advent of Integrated Energy Systems enabled various distributed energy to access the system through different power electronic devices. The development of this has made the harmonic environment more complex. It needs low complexity and high precision of harmonic detection and analysis methods to improve power quality. To solve the shortages of large data storage capacities and high complexity of compression in sampling under the Nyquist sampling framework, this research paper presents a harmonic analysis scheme based on compressed sensing theory. The proposed scheme enables the performance of the functions of compressive sampling, signal reconstruction and harmonic detection simultaneously. In the proposed scheme, the sparsity of the harmonic signals in the base of the Discrete Fourier Transform (DFT) is numerically calculated first. This is followed by providing a proof of the matching satisfaction of the necessary conditions for compressed sensing. The binary sparse measurement is then leveraged to reduce the storage space in the sampling unit in the proposed scheme. In the recovery process, the scheme proposed a novel reconstruction algorithm called the Spectral Projected Gradient with Fundamental Filter (SPG-FF) algorithm to enhance the reconstruction precision. One of the actual microgrid systems is used as simulation example. The results of the experiment shows that the proposed scheme effectively enhances the precision of harmonic and inter-harmonic detection with low computing complexity, and has good capability of signal reconstruction. The maximum detection error reaches 0.0315%, and the reconstruction signals to noise ratio (SNR) is higher than 89 dB.

Keywords: Power quality, Compressed sensing, Harmonic analysis scheme, SPG-FF algorithm

1 Introduction

In recent years, based on rising attention for environmental protection on a worldwide basis, distributed renewable energy gradually replaces conventional fossil fuel in many areas. When photovoltaic system, wind turbine and electric vehicles are connected to the grid, nonlinear power electronic devices bring serious power quality problems [1–3]. Lv, considering large-scale integration of renewable energy resources, researched the interactive energy management operation to improve the power quality [1]. Boynuegri et al. [3] studied a novel power conditioning unit to decreasing voltage distortion caused by electric vehicles. To solve the power quality problems in Integrated Energy Systems, methods with low complexity and high precision of harmonic detection and analysis have become the key technique of improving power quality in Integrated Energy Systems, especially in microgrid. Several techniques and models have been developed in recent years to address power quality issues. The methods based on wavelet packet transform [4], hanning window [5], minimize sidelobe windows [6], discrete Fourier transform (DFT) [7], as well as FFT and its improved research [8,9] have been studied and applied to the power quality analysis. These harmonic detection methods have their own characteristics, but all the typical analytic methods are based on the Nyquist/Shannon sampling theory. Their analytic methods are similar as they all begin with the collection of power quality data through high frequency

FFT and its improved research [8,9] have been studied and applied to the power quality analysis. These harmonic detection methods have their own characteristics, but all the typical analytic methods are based on the Nyquist/Shannon sampling theory. Their analytic methods are similar as they all begin with the collection of power quality data through high frequency acquisition and A/D conversion, and then this is followed by compressing the data. Although data compression can reduce the burden of transmitting mass sample data to a certain extent, a lot of hardware resources and storage space have been spent in the high-speed sampling stage before data compression. Moreover, with the development of smart grid, high frequency switch power electronic device makes harmonic components more complex and makes sampling frequencies higher, which requires more hardware resources and storage space during the Nyquist sampling process.

As a new signal processing theory, compressed sensing (CS) combines the compression process and the sampling process. The completed data compression in the sampling process can effectively reduce the utilization of hardware resources and storage space. CS has been considered for many applications including image processing [10], signal transmission [11], communication [12], etc. Although the CS theory has been applied in image processing and other fields, less research has focused on the power systems. As a promising approach, CS was discussed in connection with the application in sampling and transmitting information from large number of sensors in the smart grid communication networks, but there is no specific implementation process of the compressed sensing application [13]. In another Ref. [14], Compressive Sampling theory was employed to analyze the synchrophasor data communication in WAMS. From the description and its references, we find that "compressive sampling theory" in [14] was actually the same as "compressed sensing theory". In the literature [15], the popular CS theory was used to classify the fault area and reduce the WAN communication traffic. Another data transmission method based on compressive sensing technology was proposed in [16]. The signals were transformed into wavelet domain coefficients by means of wavelet multi-resolution analysis. Then these coefficients were sampled and wavelet inverse transforms were applied to reconstruct the original signals. Different from that in the references [15,16], this paper applies the CS theory to harmonic and inter-harmonic signal detection and fully considers the signal characteristics in electric power systems.

This paper proposes a harmonic analysis scheme based on CS technology, which can implement the function of sampling compression, signal reconstruction and harmonic detection simultaneously. Specifically, the paper mainly provides the following contributions:

(1) *Sparseness property of electrical power system harmonic signal:* The sparseness of signal is the prerequisite of using CS theory. We not only give the sparseness property of harmonic signal in electrical power system and proportion of sparseness in fundamental and harmonic components but also prove them.

(2) *Harmonics analysis scheme based on CS theory:* The scheme includes sampling process and recovery process. In the sampling process, the scheme uses the binary sparse random measurement matrix and gives the corresponding switching hardware circuit. The binary sparse measurement can effectively save the sampling storage space and reduce sampling complexity. In the recovery process, the scheme implements the function of signal reconstruction and harmonic detection simultaneously.

(3) *Spectral Projected Gradient with Fundamental Filter* (*SPG-FF*) *algorithm:* Based on the property of sparseness proportion in fundamental and harmonic components, considering the

significant differences of harmonic signal's energy in the recovery process, a novel reconstruction algorithm called the SPG-FF is proposed, which can reduce the sparsity of the signal and enhance the detection and reconstruction precision of harmonic components.

The article is structured as follows. We show how CS method can be applied to harmonic analysis. Specifically, Section 2 introduces the CS theory. The proposed harmonic analysis scheme is detailed in Section 3, followed by Section 4 describing the SPG-FF algorithm of the proposed scheme. Section 5 evaluates the proposed scheme through experiments and simulation, and Section 6 concludes the paper.

2. Compressed sensing theory

The theory of CS [17] shows that if a signal is sparse on some basis, it can be reconstructed from a small number of measurements. Even through a small number of measured values are used to solve an optimization problem, the original signal can still be reconstructed with high probability of accuracy.

To simplify the statement, the symbol x is used to define an N-dimensional non-sparse signal. If x can be represented as $x = \Psi s$ under sparse matrix Ψ, x is considered sparse. Clearly, x and s are equivalent representations of the same signal in different spaces or domains, with x in the time domain and s in the Ψ domain. The M-dimensional observation vector y can be represented as $y = \Phi x$, where Φ is an $M \times N$ measurement matrix, with $M < N$. Finally, the original signal x can be recovered accurately by the CS reconstruction algorithm. The model of CS theory is represented as

$$y = \Phi x = \Phi \Psi s = \Theta s \tag{1}$$

3. Harmonic characteristics analysis

3.1. Sparseness of harmonic signal in electrical power system

The prerequisite of using CS theory is that the original signal is sparse (named K-sparse). If the original signal x can be represented as $x = \Psi s$ under the sparse matrix Ψ, then values of most elements of coefficient vector s are less than a small positive ε, it is arguable that the original signal is a K-sparse signal.

The mathematical equation of the harmonic signal is [18]:

$$f(t) = \sum_{h=0}^{H} A_h \cos(2\pi f_h t + \varphi_h) \tag{2}$$

Here $\{A_0, f_0, \varphi_0\}$ represents fundamental component parameters, while $\{A_h, f_h, \varphi_h\}$ $(h \geqslant 1)$ represents the parameters of the harmonic component parameters, which includes Hth harmonic components. The signal has the following properties:

Property 1 (*Sparseness of harmonic signal in electrical power system*). With the Discrete Fourier Transform (DFT), the harmonic signal in electrical power system satisfies the sparseness requirements of compressed sensing

The proof is shown in Appendix A.

Property 2 (*Proportion of sparseness in fundamental and harmonic components*). In the power system, fundamental components occupy a high proportion of signal sparseness, while harmonic components occupy very low proportions.

Therefore, if the fundamental components of original harmonic signals are filtered out, the sparseness of signal K will decrease sharply.

We firstly calculate the sparseness ratio. Let α_h be the amplitude of the hth harmonic component of ($\alpha_h \ll 1$), the fundamental amplitude. In the general sparseness K of the original harmonic signal, the proportion of the fundamental sparsity K_0 is approximately equal to:

$$\left(\frac{K_0}{K}\right)_{\min} \approx \frac{1}{1 + \sum_{h=1}^{H}\alpha_h} \qquad (3)$$

The proof is shown in Appendix B.

According to standards on power quality harmonic limits GB/T14549-1993 [19], amplitudes of odd harmonics and even harmonics are within 4% and 2% of the fundamental amplitude respectively. The components of more than 12th even harmonics and 25th odd harmonics as shown in the equation below can be negligible:

$$\sum_{h=1}^{H}\alpha_h \leqslant \sum_{h=\{3,5,...,25\}}\alpha_{od} + \sum_{h=\{2,4,...,12\}}\alpha_{ev} = 12 \times 4\% + 6 \times 2\% = 0.6$$

Then $(K_0/K)_{\min} \geqslant 0.625$.

The fundamental component occupies over 62.5% in the signal sparseness. That means the sparseness can be decreased greatly if the fundamental component is filtered out from the original harmonic signals.

When $H = 5$ and $N = 2048$ in the formula (2), the signal $f(t)$ was represented by the different sparse matrices: DFT, Discrete Cosine Transform (DCT) matrix and Discrete Wavelet Transform (DWT) matrix. The degrees of sparseness under the different transform matrices were $K_{\text{DFT}} = 174$, $K_{\text{DCT}} = 185$, $K_{\text{DWT}} = 567$ respectively. The results show that the signal has better sparseness under the DFT and DCT matrix than under DWT, and the sparseness under DFT is better compared to that under DCT. Therefore, this paper employs DFT as the sparse matrix based on the theoretical analysis and numerical calculation.

3.2. Harmonic analysis scheme

The paper proposed a novel harmonics analysis scheme based on CS theory, which implements the functions of compressive sampling, signal reconstruction and harmonic detection simultaneously.

In the sampling process, using the binary sparse measurement matrix, the original N-dimensional signal x undergoes a linear reduced dimensional process to obtain an M-dimensional observation vector y ($M \ll N$). The linear reduced dimensional process reduces the usage of storage space compared with traditional Nyquist sampling schemes.

The harmonic analysis is completed in the same process as CS reconstruction in the recovery process. In order to reduce the picket fence effect and spectrum leakage problems caused by non-synchronous sampling of the inter-harmonics, we used double spectrum line interpolation algorithm in spectral line interpolation analysis, and the harmonic detection can be completed in the same process. The original reconstructed harmonics signal can be obtained from the sparse vector s with the sparse inverse transformation. The compressed sensing harmonics analysis scheme is shown in Fig. 1.

(1) Measurement matrix

This scheme uses the binary sparse random measurement matrix as a form of compression measurement matrix $\Phi^{M \times N}$ [20]. Only randomly μM elements in each column vector are set as 1,

while others are set as 0. Here μ ($\mu \ll 1$) represents the sparse ratio of the measurement matrix. The extreme sparseness of the binary sparse measurement matrix Φ greatly reduces the complexity of the compression measurement in the sampling process. Compared with traditional dense measurement methods, the complexity of CS is reduced from O(MN) to O(μMN). At the same time, the binary characteristic can be realized with just a simple switching hardware circuit, as shown in Fig. 2.

The analog information converter in the sampling process is shown in Fig. 2. $p_i(t)$ is the modulation signal emitted by the signal generator, the value of which is equal to the elemental value of row vector i in the measurement matrix. The modulation waveform $p_i(t)$ and the original signal waveform $x(t)$ are multiplied through each mixer. When the measurement matrix is the binary sparse matrix, the values of $p_i(t)$ are just 0 or 1, which means the modulation waveform is the rectangular wave. So the hardware circuit of the mixer can be easily achieved by simple analog switching or using switch transistor.

(2) Reconstruction algorithm

The compressed sensing reconstruction algorithm will directly affect the quality of reconstructed signals as well as the precision of harmonic detections. Traditional reconstruction algorithms have been well investigated, such as the Fast Iterative Shrinkage Thresholding (FISTA) algorithm, Compressed Sampling Matching Pursuit (CoSaMP) algorithm, Subspace Pursuit (SP) algorithm and Spectral Projected Gradient (SPG) algorithm [21–24]. Based on the sparseness in the fundamental and harmonic components analyzed in Property 2, this paper proposes an improved SPG algorithm, named SPG-FF algorithm, to further enhance the precision of harmonic signal reconstruction, which will be described in Section 4.

(3) Interpolation correction algorithm

To solve the fence effect and spectral leakage problems caused by simple harmonic non-synchronous sampling, this paper adopts the double spectral lines interpolation algorithm to improve the accuracy of harmonic detection.

The algorithm reduces the leakage effects by weighing the average of the maximum and the second amplitude of spectral lines in double lined interpolation, and it is the best algorithm for serious fence effects. Setting the maximum and the second spectral lines' labels of a harmonic component as k_m and k_n respectively, the correction formula for amplitude, frequency and phase angle of the double spectrum line are described as follows [26]:

$$\begin{cases} f = (k_m - 1 + \delta + 0.5)\frac{f_s}{N} \\ A = \frac{s(k_m)+s(k_n)}{N}g(\delta) \\ \varphi = angle[s(k_m + 1)] - (\delta + 0.5)\pi \end{cases} \qquad (4)$$

where,

$$\begin{cases} g(\delta) = 2.356194 + 1.155437\delta^2 + 0.326079\delta^4 + 0.078915\delta^6 \\ \delta = \frac{3(|s(k_n)| - |s(k_m)|)}{2(|s(k_n)| + |s(k_m)|)} \end{cases}$$

$$(5)$$

$s(k_m)$ and $s(k_n)$ are the k_m and k_n elements of the sparse vectors (complex vectors), respectively. $angle[s(k_m + 1)]$ is the complex angle of $s(k_m + 1)$.

4. Harmonic detection and signal reconstruction with SPG-FF algorithm

CS theory shows that the reconstruction accuracy is closely related to the signal's sparseness K, where, the smaller the value

of K, the better the reconstruction effect. The characteristics of the signals and sparse matrix are the primary influencing factors of K [17]. Property 2 shows that if the fundamental components are filtered out from the original harmonic signals, the sparseness of signal K is sharply reduced under DFT. Therefore, this paper proposed SPG-FF algorithm to enhance the reconstruction effect of harmonic signals with the filtering out of the fundamental components.

4.1. Fundamental filter (FF) algorithm

Owing to the fact that the amplitudes in the fundamental components are much larger than that of harmonic components, elements of fundamental components (including leaked spectral lines) are much larger than that of harmonic components in sparse vectors. Since the Orthogonal Matching Pursuit (OMP) reconstruction algorithm has the capability to reconstruct high energy components of sparse vectors [27], we can reconstruct the basic components by using OMP algorithm to separate them from the harmonic components.

However, when OMP algorithm is adopted to complete reconstruction of the compressed signals, the iterative terminal condition is always that the sparseness K or reconstruction error is smaller than the threshold ε ($\varepsilon \approx 0$). During each iteration, the OMP algorithm will update the support set, and the difference in support sets that determines the value of the sparse signal will be globally changed. Different from traditional OMP algorithm application, FF algorithm just needs to extract fundamental components, so it is not necessary to use the strict "threshold ε" terminal condition. But, it should not be ignored that there may be high-energy harmonic components to disturb the reconstruction process. FF algorithm is able to make improvements in iterative processes and the terminal conditions of OMP algorithms to improve the fundamental component extracting precision as follows:

(a) Establish the interference set Γ in the iterative process. The energy of the fundamental leaked line is higher than that of the harmonic spectral lines, and these spectral lines are adjacent to each other, therefore when non-zero elements of sparse estimate vectors are not adjacent to each other, they should be put into the interference set Γ.

(b) The terminal condition of iteration is based on the energy of fundamental waves. The usage of the FF algorithm is to extract and filter the fundamental components. Therefore, the terminal condition of FF algorithm is set as the percentage η of the maximum element (fundamental energy) of the estimated sparse vector, which is a positive integer relatively close to zero. Generally, when η equals to 0.1%, it can then be certain that fundamental energy has been filtered.

Because of the finite-length effect of Discrete Fourier Transforms, the elements on both sides of the maximum value in the sparse vector are not zero. Instead, it displays a trend of rapid attenuation to zero. Generally, compared with the energy of the maximum spectral line of the component, if the energy of the discrete spectrum line is very close to zero, its effect can be ignored. Therefore, when the energy of estimated sparse vectors is less than the threshold, the iteration can be terminated.

After the iteration, an estimate $\hat{s}^{base}$ of sparse vectors that only contains spectral information of the fundamental components is obtained. Its sparse inverse transform is the original reconstructed signal of fundamental components, marked as $\hat{x}^{base}$. Filtering the fundamental components, only harmonic components remains, marked as $y^{harmonic}$. To further elaborate on what has been discussed above, the FF algorithm is described below:

Algorithm: Fundamental Filter

Input: Sensing matrix $\Theta = \Phi\Psi$, Compressed harmonic signal y.

Output: Estimator of sparse vector of fundamental component $\hat{s}^{base}$, compressed signal of harmonic components $y^{harmonic}$.

Initialization: Set the number of iterations to be $t = 1$, residual $r_0 = y$, estimator of sparse vector of fundamental component $\hat{s}_0^{base} = 0$, support set $\Lambda_0 = \varnothing$, support matrix $\Omega_0 = []$, interference set $\Gamma_0 = \varnothing$, the number of Interference set elements $p = 0$

Iteration:

1. Look for index $\lambda_t = arg\,max|\Theta^T r_{t-1}|$.
2. Update support set and support matrix: $\Lambda_t = \Lambda_{t-1} \cup \{\lambda_t\}$, $\Omega_t = [\Omega_{t-1}\Theta_{\lambda_t}]$
   (Θ_{λ_t} is the λ_t column vector of sensing matrix Θ).
3. Update estimator by generalized least squares: $\hat{s}_t^{base} = \min\limits_{z:supp(z)=\lambda_t}\|y - \Omega_t z\|_2$.
4. Update residual $r_t = y - \Omega_t \hat{s}_t^{base}$.
5. If all non-zero elements of $\hat{s}_t^{base}$ are adjacent to each other, jump to step 6; else, put index of elements μ_p that are not adjacent to each other into interference set $\Gamma_p = \Gamma_{p-1} \cup \{\mu_p\}$, $p = p + 1$.
6. If all non-zero elements in $\hat{s}_t^{base}$ meet the condition $|\hat{s}_{t,i}^{base}| \geqslant \varepsilon \cdot \max\limits_{j=1,2\cdots N}|\hat{s}_{t-1,j}^{base}|$ $(i = 1, 2 \cdots \|\hat{s}_{t,i}^{base}\|_0)$, the next cycle will continue, $t = t + 1$; else, the cycle is over.

Filter:

1. Set elements of interference set index in sparse estimator $\hat{s}_t^{base}$ to zero, that is $\hat{s}_{t,\mu_i}^{base} = 0(i = 1, 2 \cdots p)$, get $\hat{s}^{base}$ estimator of fundamental sparse vector.
2. Calculate the reconstruction fundamental components $\hat{x}^{base} = \Psi\hat{s}^{base}$ and the compressed signal of harmonic components with fundamental components which are filtered out according to $y^{harmonic} = y - \Phi\hat{x}^{base}$.

Because the FF algorithm only needs to obtain the fundamental component, as compared with the OMP algorithms to accurately reconstruct signals, the iteration numbers of the FF algorithms can be greatly reduced. The recovered fundamental sparse vector $\hat{s}^{base}$, extracted by FF algorithms, contains the spectral information. Hence the fundamental signal detection of frequency, amplitude and phase can be easily completed with $\hat{s}^{base}$ interpolation correction. In this paper, double spectral line interpolation algorithm is used.

4.2. Spectral Projected Gradient (SPG) algorithm

SPG is a convex optimization method to solve the problems of BP/BPDN (Basis Pursuit/Basis Pursuit Denoise). In the algorithm, the non-monotone linear search strategy is used and spectral projected gradients and spectral steps length are set as the search direction and step length respectively. SPG has the advantages of low complexity, high reconstructed accuracy as well as good global convergence. In [25], Wang proved that SPG algorithm without any bound constraints has global convergence and finite termination, which is suitable for sparse random measurements used in this paper. Reference [23] presented the projected operator of SPG algorithm, as shown in formula (6). The searched projected gradient paths of iterations are computed by the operator in SPG algorithms.

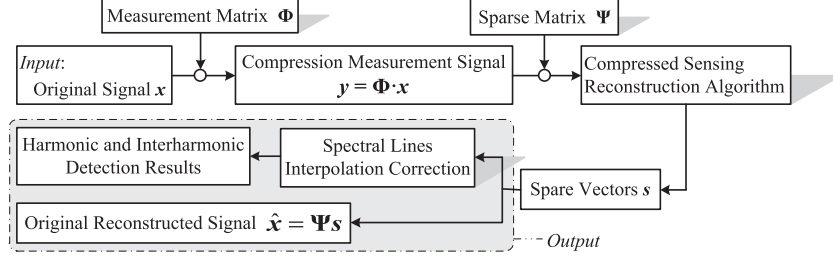$$P_\tau(c) = \underset{s.t\|x\|_1 \leqslant \tau}{\text{argmin}}\|c - x\|_2 \qquad (6)$$

Fig. 1. Harmonic analysis scheme based on compressed sensing.
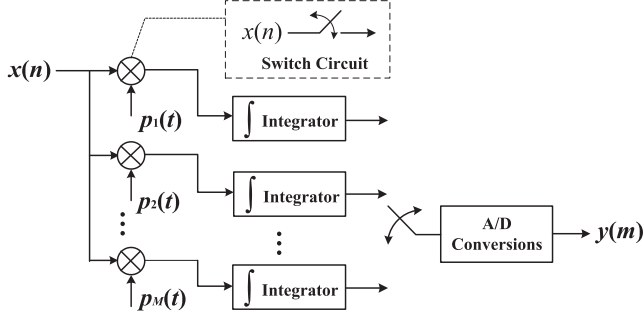

Fig. 2. Implementation of compressed sensing sampling.

The process of SPG algorithm is described as follows:

Algorithm: Spectral Projected Gradient

Initialization: Sparse estimator $\hat{s}_0^{harmonic} = 0$, residual $r_0 = y$, the initial gradient $g_0 = -\Theta^T r_0$, the initial step length $\alpha_0 \in [\alpha_{min}, \alpha_{max}]$; the number of iterations $t = 1$.

Iteration:

1. Update the current iteration estimators with linear iterative search algorithm.
   (1) Update the sparse estimators and residuals
   $\hat{s}_t^{harmonic} = P_\tau(\hat{s}_{t-1}^{harmonic} - \alpha_{t-1}g_{t-1})$; $r_t = y - \Theta\hat{s}_t^{harmonic}$
   (2) If $\|r_t\|_2^2 \leqslant \max\limits_{1 \leqslant j \leqslant \min\{t+1,L\}} \|r_{t-j}\|_2^2 + (\hat{s}_t - \hat{s}_{t-1})^T g_{t-1}$, jump to step(3); else, $\alpha_{t-1} = \alpha_{t-1}/2$, repeat step (1).
   (3) Update the gradient $g_t = -\Theta^T r_t$

2. Update spectral step length of the next iteration
   (1) $\Delta s = \hat{s}_t - \hat{s}_{t-1}$, $\Delta g = g_t - g_{t-1}$
   (2) $\alpha_t = \min\left\{\alpha_{max}, \max\left[\alpha_{min}, \frac{\Delta s^T \Delta s}{\Delta s^T \Delta g}\right]\right\}$

3. If $\|r_t\|_2 - (y^T r_t - \tau\|g_t\|_\infty)/\|r_t\|_2 > \delta$, $t = t + 1$, repeat step2; else, circulation is over, sparse estimators of harmonic component $\hat{s}^{harmonic} = \hat{s}_t^{harmonic}$.
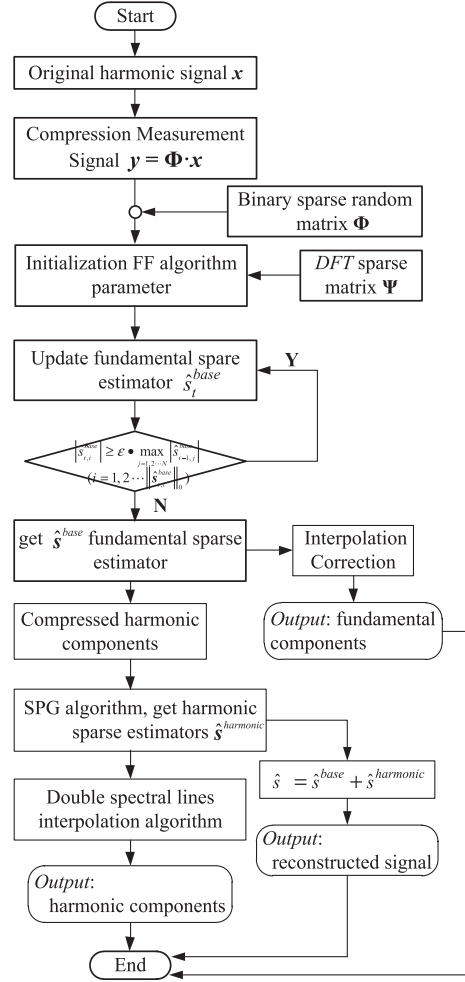

Fig. 3. Flow chart of harmonic analysis based on SPG-FF algorithm.

The whole process of compressed sensing harmonic analysis based on SPG-FF algorithm is shown in Fig. 3.

The hardware block diagram to realize the reconstruction processing is presented in the Fig. 4. It mainly includes the FF unit, matrix inversion unit, SPG unit, double spectrum line interpolation, using DSP TMS320F28335 to realize the high-speed computing. FF unit extracts fundamental component, SPG unit reconstructs harmonic and inter-harmonic components, and the real time output of harmonic detection will appear in the display device. The double spectrum line interpolation calculates the amplitude, frequency and phase angle of fundamental and harmonic components. Based on its powerful control capability, one ARM Cortex-A8 is used to manage the whole system, including the display, communication function, and other peripheral extended circuits. Through dual-access RAM, the DSP and ARM communicate with each other and realize the fast data exchange.

5. Experiment results

We performed a range of simulation experiments to test the performances of the novel harmonic analysis scheme. In order to fit the real application of integrated energy systems, in the experiment, the test power system used in this paper is the Siemens Benchmark 0.4 kV. The structure is shown in Fig. 5, which is the microgrid in connected operation mode. Fundamental frequencies of distribution networks fluctuate within 50 ± 0.2 Hz. The system contain one wind turbine (WT) which is a permanent magnet
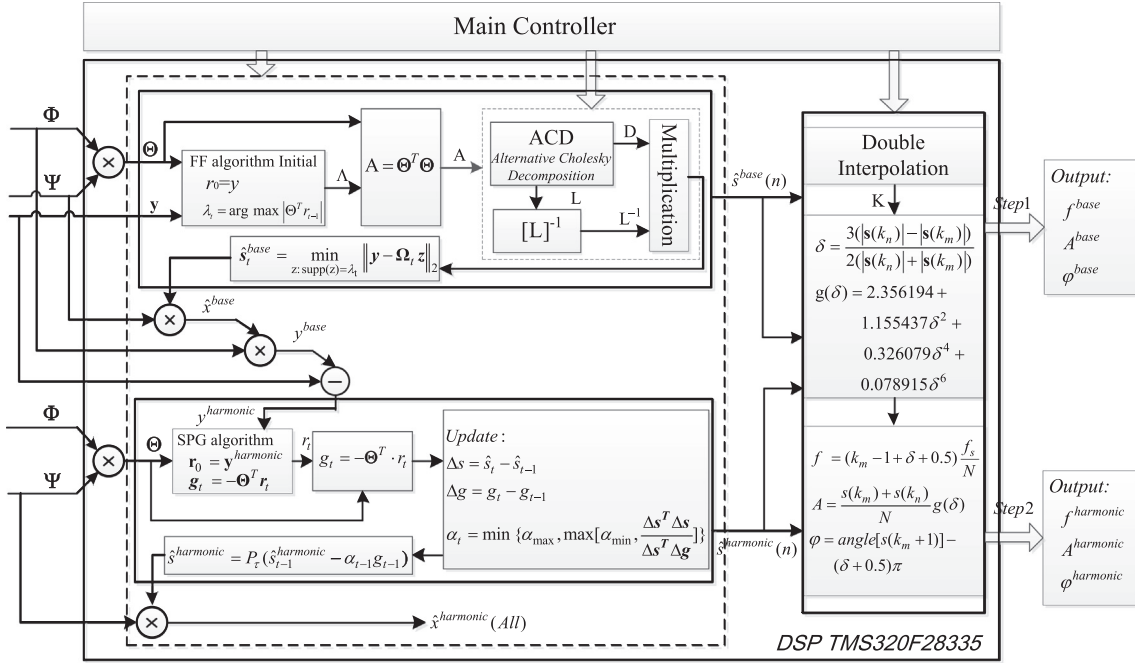
Fig. 4. Hardware block diagram of SPG-FF algorithm.
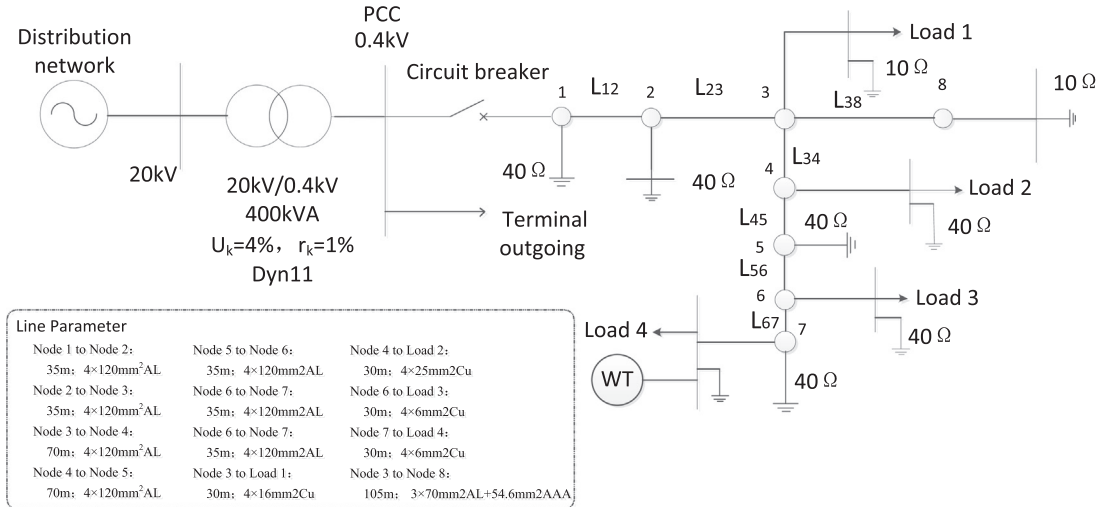

Fig. 5. Model of Microgrid.

direct-drive wind turbine using dual PWM back-to-back converters [28]. The load in microgrid is constant power load. We measured the current signals from the Point of Common Coupling (PCC), including the fundamental waves, high harmonics and inter-harmonics. The parameters are shown in Table 1.

Traditional evaluation index of harmonic analysis uses the detection precision of harmonic frequencies, amplitudes and

Table 1
Original harmonic signal.

Harmonic order	Frequency (Hz)	Amplitude (A)	Phase (°)
0.5 (Inter-harmonic)	24.9000	0.2258	17.9232
1	49.8000	39.1554	39.4610
4.8 (Inter-harmonic)	239.0400	0.1091	25.7891
5	249.0000	0.8147	27.4878
6.6 (Inter-harmonic)	328.6800	0.0808	51.3986
7	348.6000	0.4330	97.4573

phases. Besides the above three parameters in the experiments, two performance metrics were employed to evaluate the precision of compressed sampling and reconstruction algorithms: (1) Mean Squared Error (MSE) between the original signals and the reconstruction ones, (2) reconstruction signals to noise ratio (SNR), represented by

$$SNR = 10 \cdot \lg(\|\hat{x}\|_2^2 / MSE)(\text{dB}) \tag{7}$$

where $MSE = \|x - \hat{x}\|_2^2 / (M \times N)$.

5.1. Harmonic detection precision

The harmonic detection precision of frequencies, amplitudes and phases are computed to evaluate the performance of SPG-FF algorithm, in comparison with CoSaMP, SP and SPG algorithms. The results are shown in Figs. 6–8. Through the analysis of the
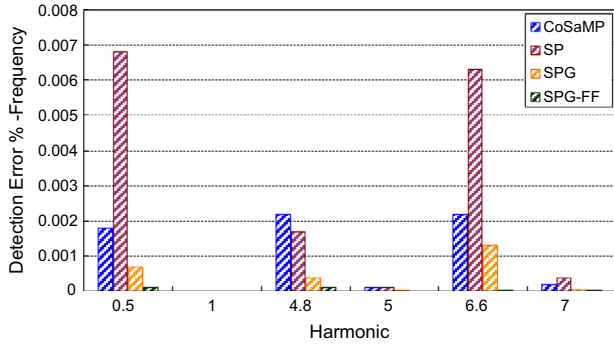
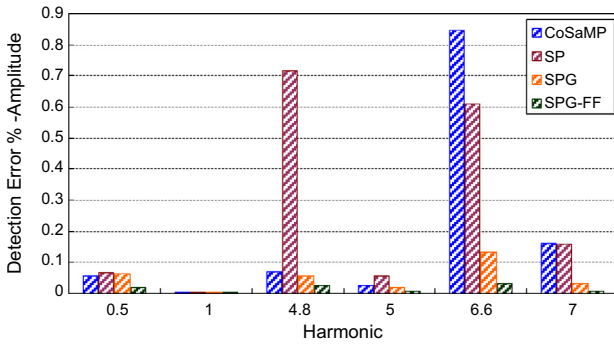**Fig. 6.** Detection error of frequency.
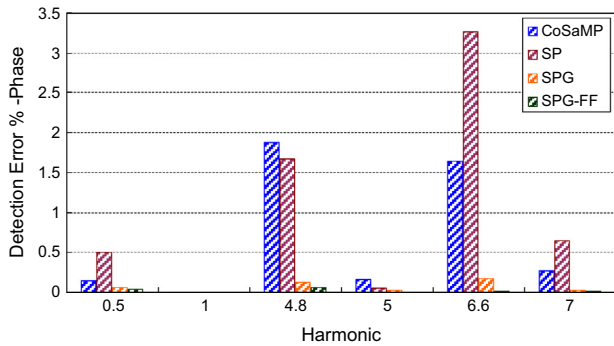

Fig. 7. Detection error of amplitude.

Fig. 8. Detection error of phase.

Fig. 9. SNR of different reconstruction algorithms.

Fig. 10. Reconstruction precision of different reconstruction algorithms.

results, SPG-FF algorithm is superior to other algorithms in terms of precision. The maximum error of the frequency, amplitude and phase are 3.04×10^{-5}%, 0.0315% and 0.0395°, respectively. This fully meets the detection precision requirements of harmonic monitoring systems. For the other three algorithms, the detection precision is very poor, especially for the CoSaMP and SP algorithms. The good performance of SPG-FF algorithm lies in decreasing the harmonic signal's sparsity K through filtering out fundamental components from the original signal.

5.2. Reconstruction precision of different reconstruction algorithm

Figs. 9 and 10 present SNR and reconstruction precision with different compression ratios. The results show that the reconstruction signals to noise ratio from SPG-FF algorithms are significantly higher than that of the other algorithms, and the reconstruction error is much lower compared to that of the other algorithms. Even in the heavy compression ratio ($M/N = 0.1$) condition, the SNR from
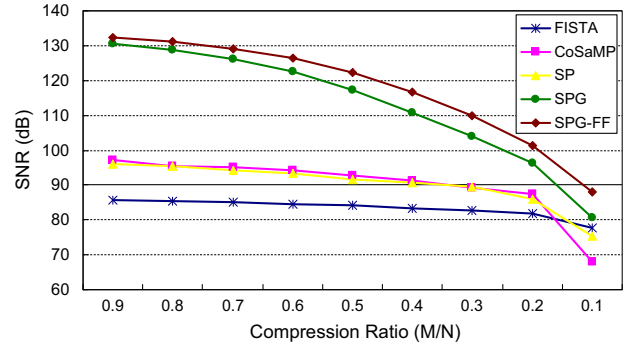
the SPG-FF algorithm can be higher than 89 dB, which can fully meet the power quality standard, such as the Chinese national standard "GB/T14549-1993 Power Quality: Public Power Network Harmonic", and the reconstruction errors are obviously lower than that of the other algorithms.

5.3. Reconstruction precision affected by different measurement matrices

Reconstruction precision affected by different measurement matrix Φ was also studied in the experiments. The reconstruction process using the same SPG-FF algorithm and the compressing sampling process using the Binary Sparse Matrix (Bi-Spa) had been studied in comparison with Gaussian Random Measurement (GSR), Parts of Hadamard Measurement (PHDM), Parts of the Fourier Measurements (PFFT), Parts of the Cosine Transform Measurement (PDCT), and Toeplitz measurement. Signal-to-noise ratio with different measurement matrices are presented in Fig. 11. The results
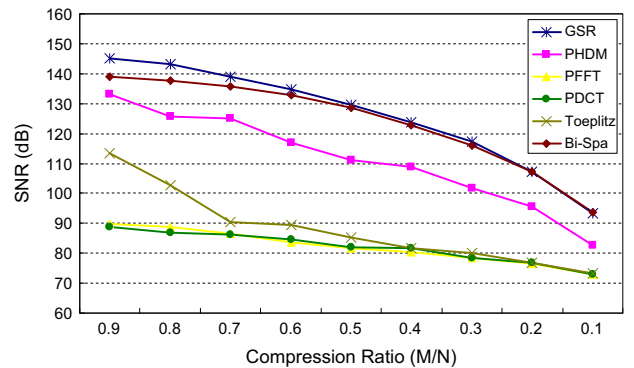

Fig. 11. SNR of different measurement matrices.

show that the SNR of the Gaussian random matrix and sparse binary measurement matrix are higher by 20–50 dB than that of the other measurement matrices.

Although GSR measurement is better than Bi-Spa measurement, and the gap is only 1 dB, it is an important observation that the Bi-Spa measurement matrix only has μMN number of nonzero elements, which greatly reduces the computing complexity in the compassing sampling process. The observation complexity is analyzed. In the sampling process, compressed sensing uses the random linear projection method to realize the compressed observation. The process can be mathematically expressed as an $M \times N$ matrix multiplied by a N column vector. Therefore, each of the observed values is computed from N times multiplication and addition operations. The observation complexity of the density matrix is O(MN). However, there are only μMN non-zero elements in the binary sparse measurement matrix. The observation complexity greatly reduces to O(μMN), $\mu \ll 1$. Therefore, the complexity for the Bi-Spa measurement is only $1/\mu$ of that for the GSR measurement.

Moreover, the hardware circuit to realize the binary transform is simpler than the non-binary ones, as shown in Section 3.2. Therefore, Bi-Spa measurement, used in this paper, is a better harmonic measurement method.

5.4. Storage burden analysis

The storage burden was evaluated in the application of the sampling framework. The CS scheme also effectively saves a large amount of hardware resources and storage space during the process of high speed sampling.

In microgrid, the monitoring system should detect not less than 25 times harmonic parameters to achieve the harmonic pollution control. The actual power quality monitoring devices can record the 50th harmonic, therefore, based on the Nyquist sampling framework, it should sample more than 100 points in one cycle. According to the standard of IEC (International Electrotechnical Commission), the detection window length takes not less than 10 cycles and each data is stored in double data types. There will be 1000 data available and it will use 8 KB of storage space for each sampling window.

For the new sampling method presented in this paper, in which the compression ratio is set to 0.1, the collected data in one cycle is 1/10 of that of the Nyquist framework. A total of only 0.8 KB storage space will be used during each sampling window. It saves a lot of storage space, and greatly reduces the transmitting load for the remote control.

6. Conclusion

This paper presented a harmonic analysis scheme based on the compressed sensing theorem, which can carry out sampling compression, signal reconstruction and harmonic detection simultaneously. As compared to the traditional harmonic detection methods based on the Nyquist sampling theorem, the proposed scheme can effectively save a large amount of hardware resources and storage space during the process of high speed sampling. The scheme selects the binary sparse measurement method to further compress the storage space, and the sampling complexity is reduced to $1/\mu$ of that of the density measurement matrix. Furthermore, this paper proposed two properties: one is the sparseness of harmonic signal in electrical power system, and the other is the proportion of sparseness in fundamental and harmonic components. Based on the property of sparseness proportion in fundamental and harmonic components, a novel SPG-FF algorithm is proposed. The results show that the SPG-FF algorithm enhances the precision

of harmonic detection and signal reconstruction, compared with that of the other four traditional algorithms.

Appendix A. The proof of the sparseness of harmonic signal in electrical power system

From formula (2), we extract any one harmonic component in the power system and discretize it under the DFT base. The sparse coefficients are:

$$F_h(k) = \sum_{n=0}^{N-1} A_h \cos\left(\frac{2\pi f_h}{f_s} n + \varphi_h\right) \cdot e^{-j\frac{2\pi}{N}nk}$$

$$= \frac{A_h}{2} e^{-j\left(\frac{N-1}{2}\right)\left(\frac{2\pi}{k} - \frac{2\pi f_h}{f_s}\right) + j\varphi_h} \frac{\sin\left(\pi k - \frac{N\pi f_h}{f_s}\right)}{\sin\left(\frac{\pi k}{N} - \frac{\pi f_h}{f_s}\right)}$$

$$+ \frac{A_h}{2} e^{-j\left(\frac{N-1}{2}\right)\left(\frac{2\pi}{k} + \frac{2\pi f_h}{f_s}\right) - j\varphi_h} \frac{\sin\left(\pi k + \frac{N\pi f_h}{f_s}\right)}{\sin\left(\frac{\pi k}{N} + \frac{\pi f_h}{f_s}\right)} = F_h^{(1)}(k) + F_h^{(2)}(k) \quad \text{(A.1)}$$

In the formula (A.1), $F_h^{(1)}(k)$ and $F_h^{(2)}(k)$ represents two symmetric spectral lines and leaked spectral line respectively. The amplitude spectra are:

$$\begin{cases} \left|F_h^{(1)}(k)\right| = \frac{A_h}{2} \left|\frac{\sin(\pi k - N\pi f_h/f_s)}{\sin(\pi k/N - \pi f_h/f_s)}\right| \\ \left|F_h^{(2)}(k)\right| = \frac{A_h}{2} \left|\frac{\sin(\pi k + N\pi f_h/f_s)}{\sin(\pi k/N + \pi f_h/f_s)}\right| \end{cases} \quad \text{(A.2)}$$

Among them, $k = 0, 1 \ldots N - 1$, we can see that when $k = \left[N\frac{f_h}{f_s}\right]$ or $k = \left[N\left(1 - \frac{f_h}{f_s}\right)\right]$, $\left|F_h^{(1)}(k)\right|$ and $\left|F_h^{(2)}(k)\right|$ reach maximum values, which are the two main spectral lines. Here, [·] is the rounding operation. Consider analyzing the amplitude spectrum of the first item $\left|F_h^{(1)}(k)\right|$, spectral line label can be set as:

$$k = N\frac{f_h}{f_s} + k' + i(i = 0, \pm 1, \pm 2 \cdots) \quad \text{(A.3)}$$

$$\left[N\frac{f_h}{f_s}\right] = N\frac{f_h}{f_s} + k'(-0.5 \leqslant k' \leqslant 0.5) \quad \text{(A.4)}$$

When $i = 0$, k represents the main line label; otherwise $|i| > 0$, k represents the leaked line label which has a distance of $|i|$ from the main line. Amplitude spectrum $\left|F_h^{(1)}(k)\right|$ can be simplified as:

$$\left|F_h^{(1)}(k)\right| = \frac{A_h}{2} \left|\sin\left(\pi k - \frac{N\pi f_h}{f_s}\right) \middle/ \sin\left(\frac{\pi k}{N} - \frac{\pi f_h}{f_s}\right)\right|$$

$$= \frac{A_h}{2} \left|\frac{\sin[\pi(k'+i)]}{\sin[\pi(k'+i)/N]}\right| = \frac{A_h C}{2} \frac{1}{|\sin[\pi(k'+i)/N]|} \quad \text{(A.5)}$$

Among them $C = \sin(\pi k')$. In the same way, set label of spectral line as $k = N\left(1 - \frac{f_h}{f_s}\right) + k' + i(i = 0, \pm 1, \pm 2 \cdots)$, $|F_h^{(2)}(k)|$ can be simplified as:

$$|F_h^{(2)}(k)| = \frac{A_h C}{2} \frac{1}{|\sin[\pi(k'+i)/N]|} \quad \text{(A.6)}$$

It can be seen that $|F_h^{(2)}(k)|$ is the same as $|F_h^{(1)}(k)|$. If the sampling point N contains the exact integer cycles of $f_h(t)$, k' equals to zero, that is $C = 0$, and amplitude of leaked spectral line is zero; if the

sampling points N contain non-integer cycles of $f_h(t)$, $k' \neq 0$, amplitude of the leaked spectral line attenuates are in the form of $\left|\frac{\sin[\pi(k'+i)]}{\sin[\pi(k'+i)/N]}\right|$, which follows the $sinc(\cdot)$ function.

Signal processing theory points out that the $sinc(\cdot)$ function has a good attenuation when $N > 100$, the energy of leaked spectral lines decay and decrease to zero rapidly. In actual harmonic monitoring systems used in power systems, the durations of data observation windows are generally 0.5–1 s, i.e., 20–100 points are acquired with each cycle to detect higher harmonic. The total sampling point $N \geqslant 1000$, which is far greater than 100. So the DFT sparse coefficients of each harmonic component $f_h(t)$ is sparse enough to satisfy the computational requirement of the compressed sensing theorem.

Appendix B. Computing the ratio formula of fundamental component sparsity K_0

In the amplitude spectrum of microgrid harmonic signals, any component's leaked spectral lines decays to zero rapidly. It can assume that when a sparse coefficient is smaller than positive ε (ε is substantially small), it is equal to 0, which means the sparseness K is decreased. Therefore, for any harmonic components $f_h(t)$, its sparseness, K_h, is the summation of i elements, which meet $|F_h^{(1)}(k)| \geqslant \varepsilon$ and $|F_h^{(2)}(k)| \geqslant \varepsilon$. The result is:

$$
\begin{aligned}
K_h &= 2 \times card\left(\left\{i \middle| \frac{A_h C}{2} \frac{1}{|\sin[\pi(k'+i)/N]|} \geqslant \varepsilon\right\}\right) \\
&= 2 \times card\left(\left\{i \middle| |i| \leqslant \frac{N}{\pi} arc \sin \frac{A_h C}{2\varepsilon} - k'\right\}\right) \\
&= 4 \times \left\lfloor \frac{N}{\pi} arc \sin \frac{A_h C}{2\varepsilon} - k'\right\rfloor + 2
\end{aligned}
\tag{B.1}
$$

where $\lfloor a \rfloor$ is rounding down a. It can be seen that the sparsity of each component is closely related to its amplitude A_h under the DFT base. In the actual power harmonic signal, the energy of the fundamental component is far higher than the energy of the harmonic components. We can assume that the amplitude of one harmonic component is α_h time of the fundamental amplitude ($\alpha_h \ll 1$). Then the sparseness K_h of harmonic component and the sparseness K_0 of fundamental component have the following relationship:

$$
\frac{K_h}{K_0} = \frac{4 \times \left\lfloor \frac{N}{\pi} arc \sin \frac{\alpha_h A_0 C}{2\varepsilon} - k'\right\rfloor + 2}{4 \times \left\lfloor \frac{N}{\pi} arc \sin \frac{A_0 C}{2\varepsilon} - k'\right\rfloor + 2} \approx \frac{arc \sin(\alpha_h A_0 C/2\varepsilon)}{arc \sin(A_0 C/2\varepsilon)} (h = 1, 2 \cdots H)
\tag{B.2}
$$

The sparseness, K_0 of fundamental components is much greater than sparseness, K_h of the harmonic component. Furthermore, the ratio of sparseness K_0 of fundamental components in the total signal's sparseness can be calculated as follows:

$$
\frac{K_0}{K} \approx \frac{K_0}{K_0 + \sum_{h=1}^{H} K_h} = \frac{arc \sin(A_0 C/2\varepsilon)}{arc \sin(A_0 C/2\varepsilon) + \sum_{h=1}^{H} arc \sin(\alpha_h A_0 C/2\varepsilon)}
\tag{B.3}
$$

where $h = 1, 2 \ldots H$ and $\alpha_h \ll 1$, $\alpha_h A_0 C/2\varepsilon \approx 0$. Therefore, $arc \sin(\alpha_h A_0 C/2\varepsilon) \approx \alpha_h A_0 C/2\varepsilon$, formula (B.3) can be simplified as:

$$
\frac{K_0}{K} \approx \frac{arc \sin(A_0 C/2\varepsilon)}{arc \sin(A_0 C/2\varepsilon) + \left(\sum_{h=1}^{H} \alpha_h\right) A_0 C/2\varepsilon} = \frac{1}{1 + \left(\sum_{h=1}^{H} \alpha_h\right) \frac{A_0 C/2\varepsilon}{arc \sin(A_0 C/2\varepsilon)}}
\tag{B.4}
$$

As $\frac{x}{arc \sin x} \in \left[\frac{2}{\pi}, 1\right]$, when $x/arc \sin x$ equals to 1, the ratio of sparseness K_0 of fundamental component in the total signal's sparseness reaches the smallest value:

$$
\left(\frac{K_0}{K}\right)_{\min} \approx \frac{1}{1 + \sum_{h=1}^{H} \alpha_h}
\tag{B.5}
$$

References

[1] Lv T, Ai Q. Interactive energy management of networked microgrids-based active distribution system considering large-scale integration of renewable energy resources. Appl Energy 2016;163:408–22.
[2] Drouineau M, Maïzi N, Mazauric V. Impacts of intermittent sources on the quality of power supply: the key role of reliability indicators. Appl Energy 2014;116(3):333–43.
[3] Boynuegri AR, Uzunoglu M, Erdinc O, et al. A new perspective in grid connection of electric vehicles: different operating modes for elimination of energy quality problems. Appl Energy 2014;132(11):435–51.
[4] Vatansever F, Ozdemir A. A new approach for measuring RMS value and phase angle of fundamental harmonic based on wavelet packet transform. Electric Power Syst Res 2008;78(1):74–9.
[5] Barros J, Diego RI. On the use of the Hanning window for harmonic analysis in the standard framework. IEEE Trans Power Delivery 2006;21(1):538–9.
[6] Wen H, Teng Z, Wang Y, et al. Simple interpolated FFT algorithm based on minimize sidelobe windows for power-harmonic analysis. IEEE Trans Power Electron 2011;26(9):2570–9.
[7] De Carvalho JR, Duque CA, Lima MAA, et al. A novel DFT-based method for spectral analysis under time-varying frequency conditions. Electric Power Systems Research 2014;108:74–81.
[8] Lin HC. Inter-harmonic identification using group-harmonic weighting approach based on the FFT. IEEE Trans Power Electron 2008;23(3):1309–19.
[9] Zeng B, Teng Z, Cai Y, et al. Harmonic phasor analysis based on improved FFT algorithm. IEEE Trans Smart Grid 2011;2(1):51–9.
[10] Patel VM, Maleh R, Gilbert AC, et al. Gradient-based image recovery methods from incomplete fourier measurements. IEEE Trans Image Process 2012;21(1):94–105.
[11] Cambareri V, Mangia M, Pareschi F, et al. A case study in low-complexity ECG signal encoding: how compressing is compressed sensing? IEEE Signal Process Lett 2015;22:1743–7.
[12] Zhao H, Li M, Wang R, et al. Compressed sensing theory-based channel estimation for optical orthogonal frequency division multiplexing communication system. Opt Commun 2014;326(5):94–9.
[13] Kayastha N, Niyato D, Hossain E, et al. Smart grid sensor data collection, communication, and networking: a tutorial. Wireless Commun Mobile Comput 2014;14(11):1055–87.
[14] Das S, Singh Sidhu T. Application of compressive sampling in synchrophasor data communication in WAMS. IEEE Trans Industr Inf 2014;10(1):450–60.
[15] Li B, He J, Yip T, et al. Wide area power system fault detection using compressed sensing to reduce the WAN data traffic. In: 2014 Sixth international symposium on parallel architectures, algorithms and programming (PAAP); 2014. p. 40–5.
[16] Yan G, Wu P. Robust data transmission upon compressive sensing for smart grid. Electric Power Comp Syst 2014;42(3):386–95.
[17] Donoho DL. Compressed sensing. IEEE Trans Inf Theory 2006;52(4):1289–306.
[18] Carranza O, Figueres E, Garcerá G, et al. Comparative study of speed estimators with highly noisy measurement signals for Wind Energy Generation Systems. Appl Energy 2011;88(3):805–13.
[19] GB/T 14549-1993: Quality of electric energy supply-Harmonics in public supply network.
[20] Gilbert A, Indyk P. Sparse recovery using sparse matrices. Proc IEEE 2010;98(6):937–47.
[21] Beck A, Teboulle M. A fast iterative shrinkage-thresholding algorithm for linear inverse problems. SIAM J Imag Sci 2009;2(1):183–202.
[22] Needell D, Tropp JA. CoSaMP: iterative signal recovery from incomplete and inaccurate samples. Appl Comput Harmon Anal 2009;26(3):301–21.
[23] Dai W, Milenkovic O. Subspace pursuit for compressive sensing signal reconstruction. IEEE Trans Inf Theory 2009;55(5):2230–49.
[24] Van Den Berg E, Friedlander MP. Probing the Pareto frontier for basis pursuit solutions. SIAM J Sci Comput 2008;31(2):890–912.
[25] Wang C, Liu Q, Yang X. Convergence properties of nonmonotone spectral projected gradient methods. J Comput Appl Math 2005;182(1):51–66.
[26] Qian H, Zhao R, Chen T. Interharmonics analysis based on interpolating windowed FFT algorithm. IEEE Trans Power Delivery 2007;22(2):1064–9.
[27] Tropp JA, Gilbert AC. Signal recovery from random measurements via orthogonal matching pursuit. IEEE Trans Inf Theory 2007;53(12):4655–66.
[28] Arifujjaman M, Iqbal MT, Quaicoe JE. Reliability analysis of grid connected small wind turbine power electronics. Appl Energy 2009;86(9):1617–23.